IEEE Access
Multidisciplinary ⋮ Rapid Review ⋮ Open Access Journal

Received 31 January 2023, accepted 19 February 2023, date of publication 23 February 2023, date of current version 22 March 2023.

Digital Object Identifier 10.1109/ACCESS.2023.3248067

RESEARCH ARTICLE

An Efficient Low Complexity Region-of-Interest Detection for Video Coding in Wireless Visual Surveillance

AHCEN ALIOUAT[1], (Student Member, IEEE), NASREDDINE KOUADRIA[1], SALIHA HARIZE[1], AND MOUFIDA MAIMOUR[2]

[1]Laboratory of Automatic and Signals of Annaba (LASA Laboratory), Faculty of Technology, Department of Electronics, Badji Mokhtar–Annaba University, Annaba 23000, Algeria
[2]CNRS, CRAN, Université de Lorraine, 54000 Nancy, France

Corresponding author: Ahcen Aliouat (ahcen.aliouat@ieee.org)

This work was supported in part by the Campus France under Grant 46082TB, and in part by the PHC TASSILI Program under Grant 21MDU323.

ABSTRACT Moving object detection (MOD) has become a popular topic in video analysis due to its use in several applications, including video coding in wireless surveillance. However, implementing MOD in constrained sensors is challenging due to their high complexity and energy consumption. Therefore, there is a great need to address the trade-off between the accuracy and the energy efficiency of MOD approaches for video coding in constrained systems. In this work, an energy-efficient region-of-interest (ROI) detection algorithm as a pre-encoder for wireless visual surveillance (WVS) is proposed. The algorithm ensures a trade-off between detection accuracy and computational complexity. To this end, we propose constructing an activity map by measuring each block activity between successive frames. The map scores are processed using a combination of a fast Gaussian smoother and a rank-order filter to improve accuracy. Only the blocks in motion are coded and counted for transmission. The accuracy of our approach has been evaluated on a large dataset using key performance metrics. It has been found that our algorithm outperforms other state-of-the-art techniques in terms of true positive rate (TPR), with 80.84% on sensitivity metric, while exhibiting a well-balanced accuracy for all categories. A careful examination of the computational complexity confirms the low overhead. The energy and bitrate savings could achieve nearly 90% and 98%, respectively.

INDEX TERMS Region-of-interest, object detection, image compression, WVS, video surveillance, energy-efficiency.

I. INTRODUCTION

Video Content Analysis (VCA) techniques involve automatically analyzing video to detect and determine spatial and temporal events. VCA is used in a wide range of domains, including video browsing and retrieval [1], image and video coding [2], [3], and video surveillance, etc. The analyze-then-compress (ATC) paradigm employs VCA to first analyze the content before compressing it. As a result, feature extraction is carried out before the compression and the transmission of the visual data captured from a visual sensor node (VS). This paradigm has been put forth as a substitute for the conventional compress-then-analyze (CTA) paradigm, which compresses the entire captured video before transmitting it to be processed further upon receipt. The CTA paradigm typically employs highly complex video coding standards [4], such as MJPEG [5], H264 [6], and HEVC [7]. Therefore, ATC can streamline this process and enable video coding within limited-resources devices [2].

The ATC paradigm [8] is well-suited for many applications [9], [10], [11] because it only compresses and transmits a few parts of the frame, known as the region-of-interest (ROI). In such applications, the end-user is only interested in the ROI, so it is relevant to extract those regions before

The associate editor coordinating the review of this manuscript and approving it for publication was Kaigui Bian.

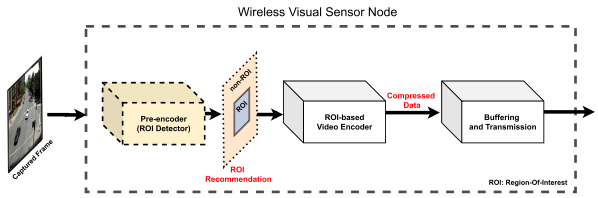

FIGURE 1. Image analysis by ROI detection for video coding in WVS.

encoding. This allows for the development and use of very low-bitrate encoders, and can result in significant savings in energy and bandwidth. Moreover, the energy consumed by the sensor node during transmission is often greater than the energy used for compression [12]. Therefore, by sacrificing some image quality and transmitting only the ROI, the bitstream can be reduced, leading to further savings in bandwidth and energy. Figure (1) illustrates the framework of this paradigm.

Despite the increased advancement in new video coding standards involving high video quality with very low bitrates, they are still not adopted for WVS [13], [14]. The unsuitability is due to the high complexity of the used coding modules, either in the intra or inter-coding modes. New approaches and paradigms have emerged to overcome this problem. They aim to code the frames based on the ROI and the difference between successive frames [15], [16]. Correspondingly, the moving object is the salient zone in the frame that must be coded, whereas non-ROI could be omitted to save bandwidth and energy in an ROI-based energy optimization approach. ROI is an important element in this context; therefore, accurate ROI detection is a crucial step that must be well-studied.

Making the tradeoff between accurate object detection and very low complexity is an important subject to be addressed and studied to advance the ROI-based video coding paradigm. To minimize contextual loss, this tradeoff must address the detection of the entire ROI (high sensitivity), but with a moderate energy budget [17], [18], [19]. Indeed, the benefit of using those approaches in video surveillance is that the cameras deployed are relatively stable, and there are few insignificant background changes. Accordingly, this topic has received a lot of attention in recent years, with numerous pre-encoder approaches proposed for video and image compression in WVS [20], [21], [22], [23].

In this work, we propose an energy-efficient pre-encoder for WVS. We combine and evaluate simple but efficient techniques that have not been addressed previously within the scope of object-based video coding for WVS. Our contribution is a proposed energy-efficient method and its detection efficiency, which we validate on a large dataset containing nearly all surveillance conditions classified into 11 categories [24]. Additionally, we validate the energy efficiency through detailed modeling of computational complexity and energy cost, to demonstrate that any neglected extra cost is outweighed by the saved energy. By avoiding unnecessarily processed and compressed blocks, the proposed pre-encoding scheme significantly reduces computational complexity.

A Block-based movIng Region Detection (BIRD) technique is proposed. BIRD detects the difference created between frames using a kind of Sum of absolute Frames Difference (SFD) [11] to address video coding in resource-constrained systems. The SFD operation is followed by heavy yet efficient morphological filtering to enhance the accuracy of the moving-region detection. A threshold is used to extract the binary mask of the moving region. The framework is considered an efficient first step in an ATC paradigm. Contrary to compressing and transmitting the whole frame (i.e., CTA), the proposed approach enables compression and transmission of only the activity blocks. This method will drastically decrease the processing and transmission energy budget in a WVS while maintaining an acceptable quality of service (QoS) and a high frame rate. The main contributions of the proposal are as follows:

- A low complexity ROI detection method dedicated to video coding in constrained wireless surveillance systems.
- The detection accuracy is improved through a combination of a fast Gaussian smoother and a rank-order filter.
- The algorithm is assessed using several metrics to evaluate the detection performance and confirm its superiority compared to the state-of-the-art techniques in constrained wireless surveillance systems.
- Bitrate and energy savings are achieved using the algorithm as a pre-encoder of a baseline JPEG compression chain.
- Based on an energy/memory consumption modeling, using ARM Cortex M3 characteristics, the viability of the algorithm is demonstrated for implementation in WVS.

The remainder of this paper is organized as follows. A background and related work review is presented in Section II. The proposed algorithm is presented in detail in Section III. Section IV shows the results and evaluation of the proposed method in terms of detection accuracy, complexity, energy, speed, and memory performance. Finally, a conclusion is drawn in Section V.

II. BACKGROUND AND RELATED WORK

The literature has extensively discussed and analyzed the design of energy-efficient Wireless Sensor Networks (WSNs) [30], [31], [32], [33]. The approaches vary depending on whether the contributions are in the processing, the transmission, or the network itself. The recommended solutions often focus on identifying resource allocation techniques that use the least amount of energy. The resource under consideration can comprise memory usage, data compression algorithms, data routing, and transmission power in the radio part.

A Wireless Multimedia Sensor Network (WMSN) integrates a camera sensor and, therefore, uses resources extensively due to the amount of multimedia data (e.g., images and video). WMSN's resources are exhausted extensively due to the amount of multimedia data (i.e.: images and video). There is a real need to reduce the amount of captured data intelligently with a minimum loss to enhance the efficiency

TABLE 1. Summary of the related work on ROI-based video coding.

Algorithm	Methodology	Highlights	Limitations
Kouadria et al. (2019) [22]	• 8 × 8 SAD • thresholding to extract ROI mask. • DTT transform for compression	• low complexity • fast image compression algorithm • dedicated to WMSN context	• less accurate • few datasets • few evaluation metrics
Rehman et al. (2016) [25]	• divide the frame into 4 blocks • select ROI from sub-blocks • background modeling • compression using DWT	• moderate accurate detection • simple and efficient algorithm • dedicated to WMSN context	• limited datasets • high bitrate • high complexity for WMSN node
Aliouat et al. (2022) [26]	• edge detection using Canny filter • 8 × 8 SAD of the edge map • automatic multi-threshold selection • multi-Otsu thresholding • compression priority to the ROI	• automatic thresholding • accurate detection • content-aware coding • allocate more resources to the ROI • dedicated to WMSN context	• high complexity • limited dataset • high bitrate (50% reduction) • no energy consumption model • few evaluation metrics
Aliouat et al. (2022) [16]	• edge detection using Sobel filter • 4 × 4 SAD of the edge map • 2-D Rank order map filtering • fixed threshold • background update each GOP	• good accuracy on the used dataset • efficient in different weather cond. • high bitrate and processing reduction • dedicated to WMSN context	• high complexity for WMSN context • limited dataset • no energy consumption model • few evaluation metrics
Ko. et al. (2018) [23]	• edge detection using Sobel filter • 8 × 8 SAD • bitrate control using PID-controller • optimal enhancement algorithm • prototyping on 130nm sensor node. • FPGA implementation	• accurate detection • optimal circuit design • high processing and bitrate reduction • dedicated to WMSN context	• limited dataset (2 sequences) • no comparison to the state of the art • few evaluation metrics
Ko. et al. (2015) [27]	• edge detection using Sobel filter • perform Frame difference • 8 × 8 SAD • rate control (channel cond. -BER-) • thresholding using PID controller	• optimal circuit design • high processing and bitrate reduction • content and energy-aware • dedicated to WMSN context	• limited dataset (4 sequences) • no comparison to the state-of-the-art • few evaluation metrics • detection accuracy not reported
Aliouat et al. (2023) [28]	• novel (S-SAD) introduced • multi-classes coding 2 based on ROI. • assessed for Human and Machine based monitoring	• accurate detection • energy model provided • high bitrate and processing saving • content-awareness • resources/quality tradeoff achieved • dedicated to WMSN context	• no detection accuracy comparison • medium dataset • fixed threshold
Sengar et al. (2020) [29]	• MOD detection suing Optical flow • Ostu for thresholding • particle swarm optimization (PSO) for redundancy exploring	• deal with moving cameras • good efficiency comparison with state-of-the-art • good rate-distortion performance	• limited dataset (4 sequences) • no energy consumption model • not dedicated to WMSN context • few evaluation metrics
BIRD (Proposed)	• 8 × 8 SFD • 1-D ROF on the activity map • FGS filter on the activity map • a pre-encoder for video coding.	• low complexity • high detection accuracy • energy modeling (ARM Cortex M3) • large dataset (51 sequences) • dedicated to WMSN context	• tested only for fixed camera • fixed threshold

of WMSN. It is essential to make a tradeoff between the added energy cost of the data reduction technique, the final gain in energy from its implementation, and the QoS degradation. Many approaches have been proposed in this context to achieve the intended target, including low-cost and classical techniques, as well as advanced techniques based on Machine Learning (ML) and deep learning [34].

One research direction in WMSN is to utilize feature extraction as a data reduction technique [35]. In [36], the authors employ the FAST and BRIEF algorithms for image

feature extraction and matching. Similarly, [8] proposes a visual feature compression method for WMSN based on the ATC paradigm. However, due to the high complexity of visual feature extraction, it is still a major drawback that the video content cannot be fully reconstructed in the pixel domain using this approach.

Movement detection is another approach used for visual data compression, where the extraction of moving objects is a crucial step. One common method involves building a background model through background subtraction (BS) to detect moving objects. Various methods are used to obtain background models, such as GMM [37], Histogram of Gradian (HoG) [38], codebook [39], ViBe [40], and deep learning-based techniques [41], [42]. However, deep learning-based techniques may not be suitable for certain special scenarios and systems, especially those with limited computing capabilities. Although the aforementioned techniques perform well in moving object detection tasks, they can be energy-intensive, making them unsuitable for use in embedded nodes.

An alternative to the aforementioned techniques is to employ simple yet efficient MOD methods, such as frame difference (FD) and BS [43], [44]. FD has been used for MOD and offers advantages such as low complexity, minimal memory usage, and fast processing speed. However, its accuracy is compromised when dealing with noisy backgrounds [31]. Edge detection (ED) has also been used to improve the efficiency of MOD algorithms, but it can be computationally expensive due to the calculations involved in the edge detection operator. Therefore, a low-cost ED operator is necessary [26], [27].

In [22], the authors proposed an ROI-based image coding technique, where only the moving blocks in the frame are detected, compressed, and sent using a low-cost compression technique involving the integer discrete Tchebichef transform. Another method has been proposed by Rehman et al. in [25], which involves dividing the frame into four main blocks and detecting the moving object in each block using a probabilistic approach. The transmission is subsequently limited to the moving segments after compression using a wavelet transform-based compression approach. In [29], the authors proposed a surveillance video compression method based on motion detection and segmentation, utilizing a JPEG-like chain for data compression.

In [16], the authors proposed an ED-based ROI detection technique using the Sobel edge detector to extract the edges of the moving regions and create an activity map based on those detected edges. In [26], the Canny ED is used as a low-cost edge detection method to extract the ROI prior to compression. ROI detection has also been a solution to control the memory usage [45], the bitrate [46], and the quality of the video encoder, accomplished by managing the bit allocation mechanisms as shown in [47]. The authors in [28] have provided a more accurate and energy-efficient strategy, in which a good trade-off between energy efficiency, image quality, content awareness, bitrate, and effective machine-based monitoring tasks at the destination have been reached. The strategy seeks to create a new pre-processing method, named Successive Sum of Absolute Differences (S-SAD) to identify the ROI and divide it into many classes based on their importance. Table 1 summarizes the related work on ROI-based video coding for WVS.

While the works mentioned above provide effective energy-saving solutions for WVS systems, many of them did not fully evaluate the efficiency of the used moving object detection methods due to limited evaluation metrics and small datasets. The presented works did not provide evidence of the effectiveness of the ROI detection techniques used. Furthermore, some methods are less efficient under WMSN constraints due to the high amount of data that must be transmitted [12]. The accuracy of the detection of the object is crucial. A lack of high detection accuracy can result in complex distortions during frame reconstruction.

The previously mentioned brief review reveals that numerous researchers are devoted to investigating ROI-based video coding in WMSN, and the techniques used produce varying degrees of accuracy and complexity. However, to the best of our knowledge, no literature validates a good accuracy-complexity tradeoff of the moving object detection techniques for ROI-based video compression in WVS. In this article, we achieve a tradeoff between accuracy and complexity through the proposed BIRD. We validate the assumptions through an application on a large dataset and an energy and memory consumption model.

III. PROPOSED METHOD

The main purpose of the BIRD method is the exploitation of the successive changes between two frames F_n and F_m, with $m < n$, where n and m are respectively the current and a previous frame in the captured video. The frame difference method is of very low complexity and simple to implement, which makes it an appropriate choice to suit the constrained resources in a WSN. Meanwhile, it suffers from low region detection accuracy [27]. To overcome the low accuracy of pixel-based detection of the frame difference method, the blocks of the resulting difference are summed up to create an activity map that represents the level of the activity in each region.

A. DIFFERENCE DETECTION

Let ϕ_n and ϕ_m be the intensity map of the frames F_n and F_m of the size $M \times N$. Based on the SFD technique [11], the summation of the non-overlapping blocks of size 8×8 for F_n is provided by Equation(1)

$$\phi_n(x, y) = \frac{1}{w^2} \sum_{u=0}^{w-1} \sum_{v=0}^{w-1} F_n(wx + u, w\,y + v), \qquad (1)$$

while for the frame F_m, ϕ_m is calculated using Equation(2)

$$\phi_m(x, y) = \frac{1}{w^2} \sum_{u=0}^{w-1} \sum_{v=0}^{w-1} F_m(wx + u, w\,y + v), \qquad (2)$$

where $x \in 0 \cdots M/w - 1$ and $y \in 0 \cdots N/w - 1$ are block indices. The resulting intensity maps ϕ_n and ϕ_m are w^2 times less than the input frame size F_n. To create the activity map Δ,

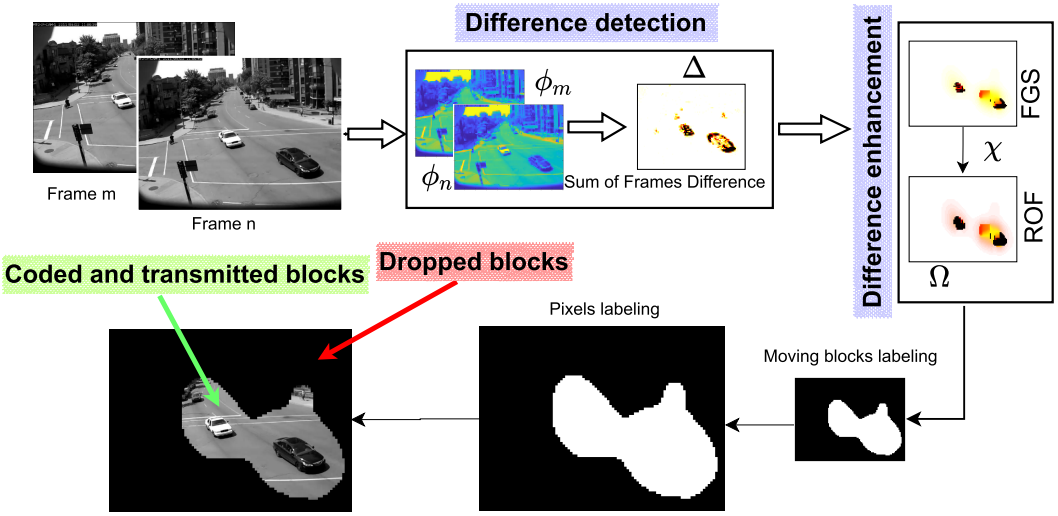

FIGURE 2. Block diagram of the proposed algorithm (BIRD).

the SFD operation is completed by computing the absolute difference between the two intensity maps, as in Equation(3)

$$\Delta(w, y) = |\phi_n(x, y) - \phi_m(x, y)| \tag{3}$$

In view of this, the scores in Δ indicate the level of activity created between the two frames. The blocks that contain high movement are represented by high score values in Δ, which indicates the moving regions. However, lower scores values indicate the non-moving regions. The complete scheme of the proposed method is shown in Figure (2).

B. DIFFERENCE ENHANCEMENT

To avoid the false negative problem and improve the accuracy, an enhancement of the scores of Δ is needed. We propose the combination of a smoothing and rank maximization of Δ. Therefore, we propose to take the advantage of both the efficiency and rapidity of the Gaussian smoother the fast global smoother (FGS) [48]. As depicted in Figure (2), FGS is applied on the Δ map to smooth the details and noisy part resulting from the SFD operation. Contrary to the convolution filters, FGS is characterized by a low complexity and rapidity estimated to be over 30 times faster than other filters. FGS uses a parameter σ to control the variance around the mean value and another parameter λ to define the amount of regularization during filtering.

Subsequently, the resulting smoothed map (χ) is filtered by the maximum rank order filter (ROF). The ROF belongs to a class of filters easy to implement [49]. The maximum rank order filter calculates the envelope of the smoothed map. It is a fast and cost-effective solution due to its simple arithmetic operations [23]. Let $Q = l_1, l_2, \cdots l_k$ be the set of input samples to the filtering process within the predefined observation window. The result of ordering the samples $l_1, l_2, \cdots l_k$ is obtained by the logical ordering $l_{(1)}, l_{(2)}, \cdots l_{(N)}$ where $l_{(i)} \in Q$, for $i \in 1 \cdots N$ represents the i^{th} order statistic. The ROF filter uses $l(N)$ the maximum order statistic. The obtained filtered map is noted Ω. Figure (3) illustrates the impact of the used filters to enhance the ROI classification performances while Figure (4) summarizes the impact of each filter as used in this order.

The binary mask is then created by comparing the Ω scores to a threshold. Where scores higher than the threshold value

Algorithm 1 The Proposed BIRD Algorithm

Input:
m selected previous frame
N SFD blocks size
K ROF window size
p rank order of the ROF
T threshold value
λ regularization of FGS
σ variance around the mean of FGS
Output:
$Mask$ binary mask of ROI
$block_{ind}$ vector of ROI blocks indexes
for *Each New frame* F_n **do**
  Apply Equations (1)(2) and (3);
  $\Delta \leftarrow SFD(F_n, F_m)$;
  Apply Fast Global Smoother ;
  $\chi \leftarrow FGS(\Delta, \lambda, \sigma)$;
  Apply 1-D Rank order filter ;
  $\Omega \leftarrow ROF(\chi, K, p)$;
  Set T;
  for *all scores in* Ω **do**
    if $Score(x, y) \geq T$ **then**
      Set $mask(block) \leftarrow 1$;
      Set $block_{ind} \in S_a$;
    else
      Set $mask(block) \leftarrow 0$;
    end
  end
  Report ROI mask to encoder ;
  Report $block_{ind}$ vector to receiver;
end

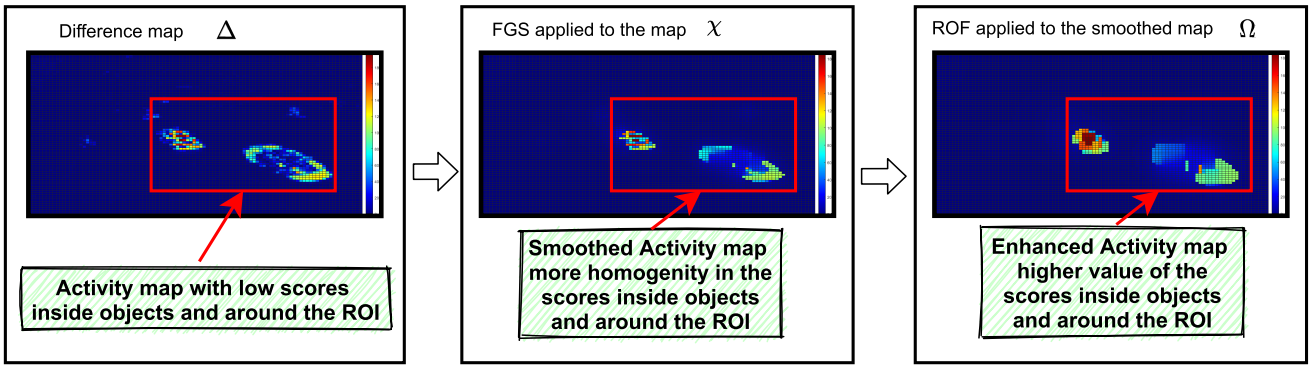

FIGURE 3. Impact of the combination of FGS and ROF on the ROI classification.

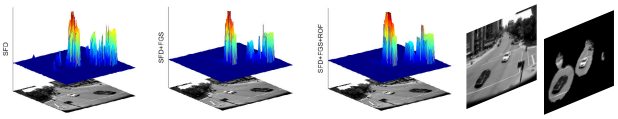

FIGURE 4. FGS eliminates unnecessary activities and ROF enhances the non-zeros scores prior to thresholding.

TABLE 2. Used parameters for the conducted simulations.

Step	SFD	FGS		ROF	
Parameter	N	σ	λ	p	K
Value	8	0.05	30	100	4

indicate activity in the associated block, whereas scores lower than the threshold value indicate inactivity.

Following the threshold operation, a set of block indices (S_a) composed of the indexes of the activity blocks is constructed. Based on the proposed strategy, only the ROI blocks will be compressed and sent to the destination. The algorithm 1 further summarizes the above steps.

IV. RESULTS AND DISCUSSION

To validate the proposed method, we present the Change Detection 2014 Dataset (CDnet) [50] results. CDnet 2014 is a very challenging dataset composed of 51 video sequences from 11 categories (more than 150000 frames + their ground truths). Since each category is associated with a specific change detection problem, e.g., dynamic background, shadows, CDnet enables an objective identification and ranking of methods that are most suitable for a specific problem as well as competent overall. The experimental values for each used parameter are summarized in Table 2.

We consider first a qualitative assessment based on visual observation of the obtained binary mask for the moving regions compared with ground truth masks.

A. PARAMETERS AND EVALUATION METRICS

Seven metrics are used for assessment. These are calculated using the confusion matrix that contains the classification characteristics in terms of quality and quantity.

1) EVALUATION METRICS

TP: True positives, the number of pixels correctly labeled as foreground.

FP: False positives, the number of pixels incorrectly labeled as foreground.

TN: True negatives, the number of pixels correctly labeled as background.

FN: False negatives, the number of pixels incorrectly set as background.

Seven measures are substituted for the preceding four in order to more accurately assess the classification results. The metrics are given by Equations (4)-(11).

Recall:

$$Re = \frac{TP}{TP + FN} \tag{4}$$

Specificity:

$$Sp = \frac{TN}{TN + FP} \tag{5}$$

Precision:

$$Pr = \frac{TP}{TP + FP} \tag{6}$$

F-measure:

$$Fm = 2\frac{Pr}{Re + Pr} \tag{7}$$

False-positive rate (FPR):

$$FPR = \frac{FP}{FP + TN} \tag{8}$$

False-negative rate (FNR):

$$FNR = \frac{FN}{TP + FN} \tag{9}$$

Percentage of wrong classifications (PWC):

$$PWC = 100\frac{(FN + FP)}{(TP + FN + FP + TN)} \tag{10}$$

Balanced-Accuracy (BAC):

$$BAC = \frac{Re + Sp}{2} \tag{11}$$

For PWC, FNR, and FPR metrics, lower values indicate higher accuracy, but for Recall, Specificity, Precision, BAC and F-Measure, higher values indicate better performance [35]. Recall gives the percentage of necessary

TABLE 3. Samples of ROI extraction mask results.

Sequence	Original	ground-truth	mask	ROI
Highway #1475				
SnowFall #2784	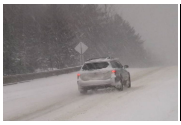			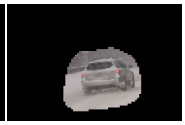
Pedestrians #476		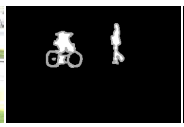		
Blizzard #1406	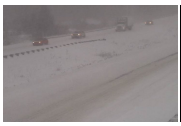			
WinterDriveway #1860				
tunnelExit #2329				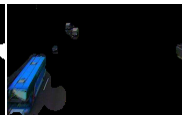
Sofa #1185	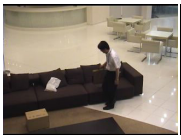			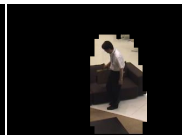
PTZ #1240				
Park #250		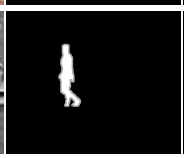	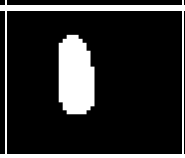	
NightVideo #1300	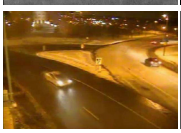			
Busstation #400				
Turbulance0 #2045				

positives via the compared total number of true positive pixels in the ground truth. Precision gives the percentage of unnecessary positives through the compared total number of positive pixels in the detected binary objects mask.

Among these metrics, we are specifically interested in the recall and balanced-Accuracy metrics (BAC). ROI-based video coding needs a high TP with a minimum FN. Advanced analysis is performed by exposing the TPR-FPR curve

TABLE 4. Detection results of the proposed algorithm over CDnet 2014 dataset.

Category	Recall	Specificity	FPR	FNR	PBC	Precision	F-Measure
PTZ	0.9662	0.6443	0.3556	0.0337	35.3016	0.0401	0.0753
badWeat.	0.9208	0.8948	0.1051	0.0791	10.1795	0.2747	0.3904
baseline	0.7619	0.9437	0.0562	0.2380	6.6360	0.3268	0.4047
cameraJ.	0.8504	0.6446	0.3553	0.1495	34.5590	0.1383	0.2238
dynamic.	0.7593	0.9512	0.0487	0.2406	4.9399	0.1962	0.2801
intermi.	0.4186	0.8603	0.1396	0.5813	16.4228	0.1566	0.2242
lowFram.	0.8161	0.7905	0.2094	0.1838	20.2242	0.1315	0.1919
nightVi.	0.9455	0.8374	0.1625	0.0544	15.9206	0.1193	0.2108
shadow	0.8775	0.8500	0.1499	0.1224	14.8039	0.2416	0.3740
thermal	0.7548	0.8894	0.1105	0.2451	13.4618	0.3575	0.4095
turbule.	0.8216	0.8870	0.1129	0.1783	11.3767	0.1000	0.1607
Overall	0.8084	0.8357	0.1642	0.1915	16.7115	0.1893	0.2678

TABLE 5. Comparison of BIRD with classical techniques over CDnet 2014 dataset.

Technique	Recall	Specificity	FPR	FNR	PWC	F-Measure	Precision
KNN [51]	0.6650	0.9802	0.0198	0.3350	3.3200	0.5937	0.6788
GMM1 [52]	0.6846	0.9750	0.0250	0.3154	3.7667	0.5707	0.6025
KDE [53]	0.7375	0.9519	0.0481	0.2625	5.6262	0.5688	0.5811
MahaD [54]	0.1644	0.9931	0.0069	0.8356	3.4750	0.2267	0.7403
GMM2 [55]	0.6604	0.9725	0.0275	0.3396	3.9953	0.5566	0.5973
EucD [54]	0.6803	0.9449	0.0551	0.3197	6.5423	0.5161	0.5480
BIRD	0.8084	0.8357	0.1642	0.1915	16.7115	0.1893	0.2678

(ROC curve) for sample sequences with an analysis of the optimum threshold.

B. PERFORMANCES OF BIRD OVER THE CDnet 2014

Table 3 shows the performance of BIRD indicating the algorithm's visual accuracy in detecting all the ROI candidates for compression and transmission. The presented sample frames from all categories of the benchmark dataset in Table 3 show that the algorithm successfully detects the blocks in which a high movement occurs. Objects are entirely detected in most videos, which could be a good enabler for a variety of applications, especially as a pre-encoder for ROI-based video coding [23].

It should be noted that, for some video scenarios (like the *Office* video sample), the algorithm is unable to detect the target object for some time due to the object's stability. Even though the object information has already been delivered to the destination, the reported numerical results are reduced.

Table 4 shows the quantitative results on CDnet 2014 dataset. The results indicate the good performance of the proposed algorithm in the detection of the whole object with high TP values for different categories. The algorithm shows high detection results for some categories and moderate detection performances for others. For example, the recall metric is high for almost all the categories but shows exceptional performance for night video and dynamic background, PTZ, and camera jitter categories despite their difficult scenarios. The algorithm presents some weaknesses in detecting the complete object in some categories like intermittent object motion category.

C. COMPARISON WITH OTHER TECHNIQUES

Table 5 shows the overall results of our method on CDnet 2014 dataset compared with the state-of-the-art techniques, namely KNN in [51], GMM in [52], KDE in [53],

TABLE 6. Category-wise comparison of BIRD with the state-of-the-art on CDnet 2014 dataset.

Category	Recall			Specificity			Balanced Acc.		
	BIRD	Savas [56]	Cwizar [24]	BIRD	Savas [56]	Cwizar [24]	BIRD	Savas [56]	Cwizar [24]
Dynamic.	0.7593	0.6436	0.8144	0.9512	0.9962	0.9985	0.8553	0.8199	0.9064
PTZ	0.9662	0.7685	0.3833	0.6443	0.9977	0.9968	0.8053	0.8831	0.6901
BadWeat.	0.9208	0.5647	0.6697	0.8948	0.9985	0.9993	0.9078	0.7816	0.8345
Baseline	0.7619	0.6214	0.8972	0.9437	0.8213	0.9980	0.8528	0.7213	0.9476
CameraJ.	0.8504	0.4567	0.7436	0.6446	0.9788	0.9931	0.7475	0.7177	0.8683
Intermi.	0.4186	0.5547	0.8324	0.8603	0.9979	0.9911	0.6394	0.7763	0.9118
LowFram.	0.8161	0.5490	0.6659	0.7905	0.7464	0.9949	0.8033	0.6477	0.8304
nightVi.	0.9455	0.4593	0.4511	0.8374	0.9583	0.9874	0.8915	0.7088	0.7193
Shadow	0.8775	0.8365	0.8786	0.8500	0.9828	0.9910	0.8638	0.9097	0.9348
Thermal	0.7548	0.4650	0.7268	0.8894	0.9647	0.9949	0.8221	0.7148	0.8609
Turbule.	0.8216	0.7421	0.7122	0.8870	0.9883	0.9997	0.8543	0.8652	0.8559
Overall	0.8084	0.6056	0.6608	0.8357	0.9483	0.9948	0.8220	0.7770	0.8509

*bold values are the best category-wise, red values are the best overall, blue values are the second best

Mahalanobis Distance and Euclidean Distance techniques presented in [54], and another GMM-based technique in [55]. The proposed method exhibits good results in the recall and FNR metrics with the best results against other techniques and shows competitive results for the specificity metric. The weaknesses of the algorithm in the precision and F-measure values (0.1893 and 0.2678) can be explained by the adopted block-based techniques, which allow the detection of additional pixels with the moving object, resulting in high FPR. According to 4, the results of BIRD are considered very high in the context of studies that aim to integrate object detection as a pre-processing step for WVS in very low-complexity platforms.

D. METRICS OF INTEREST: RECALL, SPECIFICITY AND BAC

A balance between the TP and FN is important to measure the performance of BIRD in detecting the complete object while avoiding the drawback of non-detection of regions inside the moving objects and with a minimum FP possible. We compare BIRD to two methods, one method uses Neural Networks for object detection [24]. The second method uses block-based object detection [56] same as our proposed method.

As presented in Table 6, the BAC and recall metrics of BIRD show higher values than in [56] for most of the sequences. While [24] shows superior BAC and specificity values compared with BIRD and [56]. Results of BIRD are still very competitive to that of [24]. With an overall BAC of 82%, BIRD can ensure high detection accuracy of the moving object regions for different categories and conditions.

E. THE IMPACT OF THRESHOLDING ON DETECTION

We have selected three sequences from the used dataset to empirically validate the accuracy and low-overhead assumptions of BIRD. the *Highway* sequence with a size of (320 × 240) contains high activity with a number of moving vehicles, while the *pedestrians* sequence of size (360 × 240) is of low activity with relatively high stability in the background. The *Snowfall* sequence of size (720 × 480) is a long sequence that contains moving objects with very high activity in the background (Snow and winter).

In Figure (5) we plot the TPR against the FPR when varying the threshold value from 0 to 10. The obtained ROC curves show that low thresholds imply a high true positive rate, but this adversely affects the specificity of the detection since more data is wrongly labeled as activity blocks, which means that more data is to be considered for delivery. The optimum threshold that allows the best tradeoff between TPR and FPR could be achieved, as shown by the orange dots in each ROC curve. It is defined by calculating the minimum Gaussian distance between the results of TPR and FPR: $min(\sqrt{(1-sensitivity)^2+(specificity-1)^2})$.

Figure (6) shows the impact of varying the threshold value on the mean value of the detected blocks. In the case where high stability characterizes the background (for example *pedestrians* sequence), a high threshold is generally preferred since there is a low risk of wrongly including background

TABLE 7. Statistics of the energy gain under threshold variation.

Threshold	Highway			Pedestrians			Snowfall		
-	mean (ROI)$_{(ceiled)}$	ratio (ROI)	Δ energy (theoretically)	mean (ROI)	ratio (ROI)	Δ energy (theoretically)	mean (ROI)	ratio (ROI)	Δ energy (theoretically)
10	149	12.41%	+87.59%	49	03.63%	+96.37%	68	01.26%	+98.74%
9	160	13.33%	+86.67%	52	03.85%	+96.15%	74	01.37%	+98.63%
7	192	16.00%	+84.00%	60	04.44%	+95.56%	87	01.61%	+98.39%
5	249	20.75%	+79.25%	76	05.63%	+94.37%	110	02.04%	+97.96%
3	291	24.25%	+75.75%	120	08.89%	+91.11%	190	03.52%	+96.48%
1	621	51.75%	+48.25%	273	20.22%	+79.78%	1857	34.39%	+65.61%
0	1003	83.58%	+16.42%	598	44.30%	+55.70%	4360	80.74%	+19.26%
Max	1200	100%	-	1350	100%	-	5400	100%	-

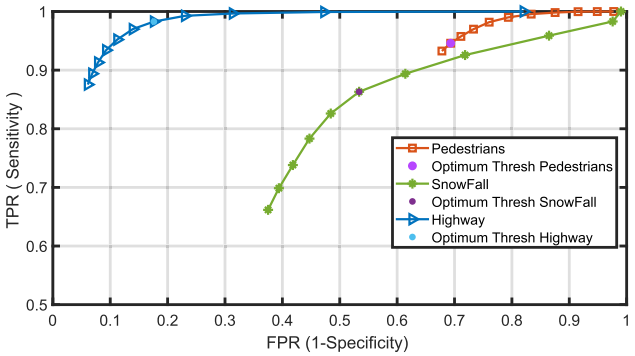

FIGURE 5. ROC curve and the optimum threshold for *pedestrians*, *Highway* and *Snowfall* sequences.

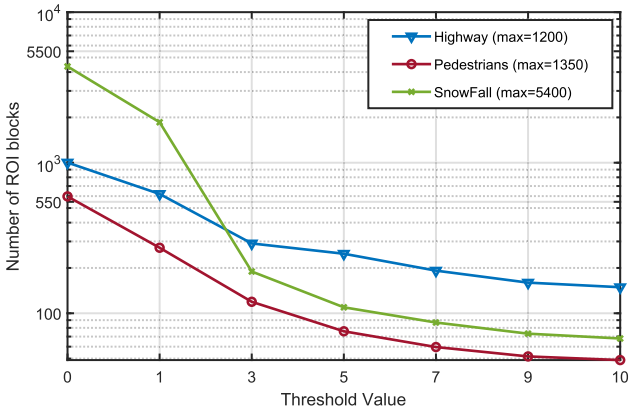

FIGURE 6. Number of blocks belonging to the ROI according to the threshold value.

blocks in the ROI. Meanwhile, a high number of background blocks is classified as ROI in the case of noisy and dynamic background (the Snowing scene in the *Snowfall* sequence for example). A higher number of the ROI detected blocks may enhance the quality of the reconstructed frames at the destination. But, at the cost of higher energy and bitrate.

Table 7 shows the impact of the threshold value on the energy gain expressed by the number of skipped blocks. From the table, it can be seen that the mean number of ROI blocks is inversely proportional to the threshold value. As a result, the energy gain is low when the chosen threshold value is low. A borderline case is when the threshold value is 0 (i.e.the activity score is absolutely greater than 0), which gives the lowest energy gain. The row that begins with MAX, indicates that all the frame's blocks will be compressed and transmitted (i.e.including the blocks in which the activity score is equal to 0). In this case, all the frame's blocks are taken into account for compression and transmission, rendering the method ineffective. According to the accuracy results shown in Figure 5, for the *pedestrians* sequence, the optimum threshold for good detection accuracy is 9. Consequently, this threshold value enables a saving of about 96% of the processing and transmission energy compared to the CTA approach (Table 7). Choosing a low threshold value is without benefit to the surveillance system, while an optimum threshold could significantly save the energy consumption in the sensor node and the bitrate needed for transmission. Furthermore, an optimum threshold enables the optimum ratio of the activity blocks and could be used as a rate controller, which is an interesting subject for future work.

F. METHOD COMPLEXITY

To evaluate the energy consumption on embedded sensor conditions, we have considered a sensor node equipped with an ARM Cortex M3 micro-controller [57]. Table 8 shows the characteristics of the processor.

Using MATLAB 2020a and C++ running on a PC intel Core i7-2670QM 2.2Ghz, with 8GB RAM on Windows 7 OS, 2.6 ms to process one frame of 320240 is recorded allowing processing of 384 frames per second (fps).

TABLE 8. ARM cortex M3 characteristics.

Sensor Processor	Cortex M3
Clock rate	72 MHz
Processor power	23 mW
Cycles count	Add.[1], Sub.[1], Mult.[1 or 2], Div.[1 to 12].

1) ENERGY BUDGET FOR CHANGE DETECTION

The total energy budget of the proposed BIRD algorithm is directly proportional to its computational complexity and could be expressed as follows:

$$E_{Detection} = E_{SFD} + E_{FGS} + E_{ROF} + E_{Threshold} \quad (12)$$

The total computational budget of the method is presented in Table 9. The number of operations for FGS is reported in [48], while the ROF budget is $R = K(K-1)/2$, where K is set to 4 for the proposed method and represents the size of the sliding vector. The filter uses the sliding vector over the columns. After each calculation step, the vector is shifted by one position down, and the operation is executed till the end of the line vector. This process is performed along all the columns. For $K = 4$, the ROF performs 6 comparisons for each score value in the map.

Since the number of operations performed is proportional to the frame size and the block size ($8 \times 8, 16 \times 16 \cdots$), a generalized model of the number of arithmetic operations should be presented. We present in Table 9 the number of operations for each step in terms of frame size (N, M) and block size(w). Table 9 also shows the energy budget of each step and the total energy budget of the BIRD. Table 10 shows a comparison of the energy budget of the proposed object detection method against state-of-the-art techniques for 240 $\times$ 320, namely MoG [52], CS-MoC [58], CoSCS-MoG [59], EBSCAM [60] and the basic FD technique. The proposed technique shows the lowest energy consumption records in both its minimal and maximal cases. While energy consumption recorded an increase of about 38% compared to FD when extreme cases are considered.

2) ENERGY DISSIPATION FOR COMPLETE COMPRESSION CHAIN

Considering a complete compression chain, the total in-node processing budget could be expressed as follow:

$$E_{total} = E_{Detection} + E_{compress}, \quad (13)$$

where $E_{Detection}$ is the energy cost of the object detection part as presented by Equation (12), $E_{compress}$ is the energy cost of the compression part. For the calculation of $E_{compress}$, the model has been studied and provided in [61] under the same conditions.

The compression cost for each frame includes the DCT compression, the quantization cost and the Huffman coding cost. Three implementations of the JPEG-based compression are shown in [61], namely float IJG, slow IJG, and fast IJG. In this work, the slow IJG implementation is adopted with an energy cost of $192.28\mu J$ for each 8×8 block.

Since N_{blocks} represents the number of activity blocks detected that will be coded for each frame, the compression cost is proportionally related to N_{blocks}. For example, the *Highway* sequence incurs an overhead of the object detection step $E_{Detection}$ equal to 0.6891 $mJ/frame$.

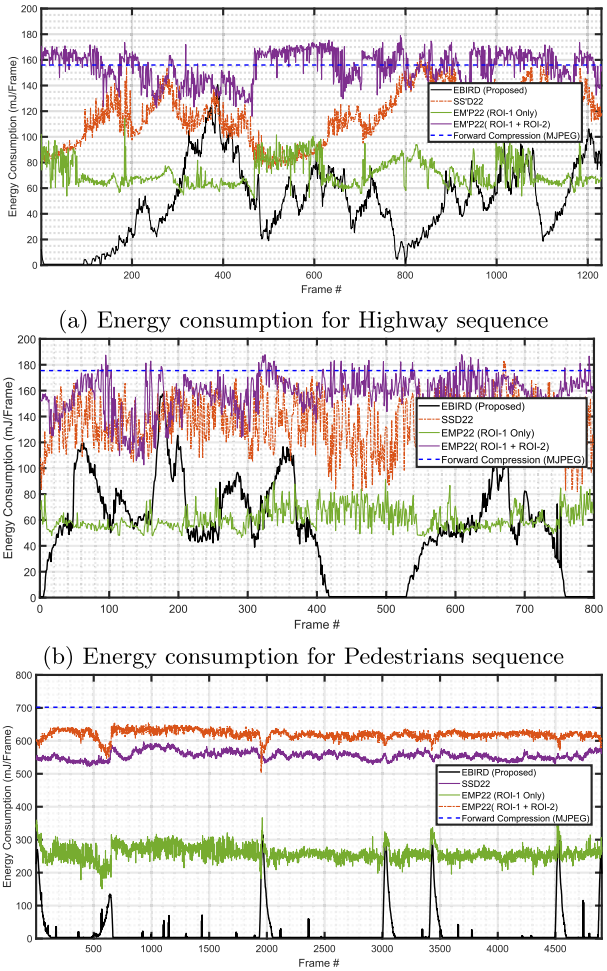

(a) Energy consumption for Highway sequence

(b) Energy consumption for Pedestrians sequence

(c) Energy consumption for snowfall sequence

FIGURE 7. Per-frame energy dissipation of BIRD for *Highway*, *pedestrians* and *Snowfall*.

Figure (7) illustrates the per-frame energy consumption of the proposed method compared to ROI-based compression methods, namely, [26] referred to as EMP'22, [16] referred to as SSD'22 and the forward baseline compression (MJPEG). Since the algorithm is applied to each frame, constant energy is spent for each frame, while the total energy curves oscillate based on the number of blocks to compress. BIRD shows the best results as the lowest energy budget for all the scenarios.

The energy dissipation of the BIRD method is proportional to the frame size. About 79.29% of blocks are skipped for the *Highway* sequence compared to the standard coding (MJPEG for example), while more than 98% of the blocks are skipped for *SnowFall* sequence and 86.89% for *pedestrians* sequence. The level of energy consumption at the processing step is correlated with the number of skipped blocks.

Although the other techniques have good ROI detection, they are hindered by the high energy cost of the detection step. This is because of the use of computationally

TABLE 9. Computational budget of each step of BIRD algorithm.

Step	Operations	# of Operations	Energy consumption (mJ/Frame) min ($Cycles_{div} = 1$)	max($Cycles_{div} = 12$)
SFD	Addition	$NM - NM/w^2$	0.2693	0.4
	Subtraction	NM/w^2		
	Absolute	NM/w^2		
	Division	NM/w^2		
ROF	Comparison	$6(N/w^2 - 3)M/w^2$	$7.4250e^{-5}$	$7.4250e^{-5}$
FGS	Multiplication	$6NM/w^2$	0.0832	0.2851
	Division	NM/w^2		
Thresholding	Comparison	NM/w^2	0.004	0.004
$E_{detection}$	-	-	0.3723	0.6891

TABLE 10. Per-frame $E_{detection}$ cost of the method compared to state-of-the-art for size (240 × 320).

Method	Energy Budget (mJ/Frame)	
	min ($Cycles_{div} = 1$)	max ($Cycles_{div} = 12$)
MoG [52]	649.95	
CS-MoG [58]	116.44	
CoSCS-MoG [59]	125.96	
EBSCAM [60]	3.4	
FD	0.5069	
BIRD (proposed)	0.3723	0.6891

expensive edge detection and automatic thresholding techniques in [16], [26], respectively, which involve arithmetic convolution and histogram calculation. However, optimizing the design of edge detectors and Otsu's threshold can help optimize their energy cost.

Figure (7) demonstrates that the algorithm is highly efficient in conserving processing and transmission power, saving more than 90% of energy most of the time. The proposed method strikes a good balance between energy savings and detection accuracy.

3) MEMORY REQUIREMENTS

We analyze here the memory requirement of the proposed region detection method. The method requires storing the previous grayscale frame of 8-bit depth and updating every frame, corresponding to a memory of $N \times M$ bytes. Two score maps are to be stored which requires a memory of $2 \times N \times M/w^2$ bytes. The ROF and the FGS filters are performed locally on the stored activity map. Thus, the needed memory for these operations is ignored (window of 4 Bytes for ROF and short vectors for FGS). For $w = 8$, the total memory consumption is about 1.031 bytes per pixel.

V. CONCLUSION

In this study, we proposed an energy-efficient approach for detecting moving regions as a pre-encoder for WVS. The suggested approach is based upon a low-complexity SFD operation followed by morphological filtering and thresholding. The proposed method's overall efficiency was evaluated using a standard dataset as a benchmark. The performance assessment shows a satisfactory balance between the proposed method's detection accuracy, energy efficiency, and memory. In these respects, our approach effectively

relieves the burden of processing and compressing video sequences for resource-constrained surveillance devices. However, the proposed method has two main drawbacks: (1) It has only been tested on fixed cameras, and (2) In some cases, it produces poor results using certain performance metrics, like F-measure, due to its commitment to meeting the constrained of WVS. Future studies should focus on improving the algorithm's performance and implementing it in an embedded WVS system, taking into account channel/network conditions.

REFERENCES

[1] S. H. Abdulhussain, A. R. Ramli, M. I. Saripan, B. M. Mahmmod, S. A. R. Al-Haddad, and W. A. Jassim, "Methods and challenges in shot boundary detection: A review," *Entropy*, vol. 20, no. 4, p. 214, Mar. 2018.

[2] A. Redondi, L. Baroffio, L. Bianchi, M. Cesana, and M. Tagliasacchi, "Compress-then-analyze versus analyze-then-compress: What is best in visual sensor networks?" *IEEE Trans. Mobile Comput.*, vol. 15, no. 12, pp. 3000–3013, Dec. 2016.

[3] A. Redondi, L. Baroffio, M. Cesana, and M. Tagliasacchi, "Compress-then-analyze vs. analyze-then-compress: Two paradigms for image analysis in visual sensor networks," in *Proc. IEEE 15th Int. Workshop Multimedia Signal Process. (MMSP)*, Sep. 2013, pp. 278–282.

[4] I. Mansri, N. Doghmane, N. Kouadria, S. Harize, and A. Bekhouch, "Comparative evaluation of VVC, HEVC, H.264, AV1, and VP9 encoders for low-delay video applications," in *Proc. 4th Int. Conf. Multimedia Comput., Netw. Appl. (MCNA)*, Oct. 2020, pp. 38–43.

[5] S. Fossel, G. Fottinger, and J. Mohr, "Motion JPEG 2000 for high quality video systems," *IEEE Trans. Consum. Electron.*, vol. 49, no. 4, pp. 787–791, Nov. 2003.

[6] *Advanced Video Coding for Generic Audiovisual Services*, document ITU-T Recommendation H. 264, 2003.

[7] S. Harize, A. Mefoued, N. Kouadria, and N. Doghmane, "HEVC transforms with reduced elements bit depth," *Electron. Lett.*, vol. 54, no. 22, pp. 1278–1280, Nov. 2018.

[8] L. Baroffio, M. Cesana, A. Redondi, M. Tagliasacchi, and S. Tubaro, "Coding visual features extracted from video sequences," *IEEE Trans. Image Process.*, vol. 23, no. 5, pp. 2262–2276, May 2013.

[9] A. Boulmaiz, N. Doghmane, S. Harize, N. Kouadria, and D. Messadeg, "The use of WSN (wireless sensor network) in the surveillance of endangered bird species," in *Advances in Ubiquitous Computing*. Amsterdam, The Netherlands: Elsevier, 2020, pp. 261–306.

[10] A. Sakhri, O. Hadji, C. Bouarrouguen, M. Maimour, N. Kouadria, A. Benyahia, E. Rondeau, N. Doghmane, and S. Harize, "Audio-visual low power system for endangered waterbirds monitoring," *IFAC-PapersOnLine*, vol. 55, no. 5, pp. 25–30, 2022.

[11] L. Kong and R. Dai, "Efficient video encoding for automatic video analysis in distributed wireless surveillance systems," *ACM Trans. Multimedia Comput., Commun., Appl.*, vol. 14, no. 3, pp. 1–24, Aug. 2018.

[12] S. Soro and W. Heinzelman, "A survey of visual sensor networks," *Adv. Multimedia*, vol. 2009, pp. 1–21, May 2009.

[13] Z. Pan, L. Chen, and X. Sun, "Low complexity HEVC encoder for visual sensor networks," *Sensors*, vol. 15, no. 12, pp. 30115–30125, Dec. 2015.

[14] X. Jiang, J. Feng, T. Song, and T. Katayama, "Low-complexity and hardware-friendly H.265/HEVC encoder for vehicular ad-hoc networks," *Sensors*, vol. 19, no. 8, p. 1927, Apr. 2019.

[15] M. Maimour, "SenseVid: A traffic trace based tool for QoE video transmission assessment dedicated to wireless video sensor networks," *Simul. Model. Pract. Theory*, vol. 87, pp. 120–137, Sep. 2018.

[16] A. Aliouat, N. Kouadria, M. Maimour, and S. Harize, "Region-of-interest based video coding strategy for low bitrate surveillance systems," in *Proc. 19th Int. Multi-Conf. Syst., Signals Devices (SSD)*, May 2022, pp. 1357–1362.

[17] M. A. Hossain, M. I. Hossain, M. D. Hossain, and E.-N. Huh, "DFC-D: A dynamic weight-based multiple features combination for real-time moving object detection," *Multimedia Tools Appl.*, vol. 81, no. 22, pp. 1–32, 2022.

[18] H. Wei and Q. Peng, "A block-wise frame difference method for real-time video motion detection," *Int. J. Adv. Robotic Syst.*, vol. 15, no. 4, Jul. 2018, Art. no. 172988141878363.

[19] B. Laugraud, S. Piérard, M. Braham, and M. Van Droogenbroeck, "Simple median-based method for stationary background generation using background subtraction algorithms," in *Proc. Int. Conf. Image Anal. Process.* Cham, Switzerland: Springer, 2015, pp. 477–484.

[20] L. Kong and R. Dai, "Object-detection-based video compression for wireless surveillance systems," *IEEE MultimediaMag.*, vol. 24, no. 2, pp. 76–85, Apr. 2017.

[21] L. Galteri, M. Bertini, L. Seidenari, and A. Del Bimbo, "Video compression for object detection algorithms," in *Proc. 24th Int. Conf. Pattern Recognit. (ICPR)*, Aug. 2018, pp. 3007–3012.

[22] N. Kouadria, K. Mechouek, S. Harize, and N. Doghmane, "Region-of-interest based image compression using the discrete tchebichef transform in wireless visual sensor networks," *Comput. Electr. Eng.*, vol. 73, pp. 194–208, Jan. 2019.

[23] J. H. Ko, T. Na, and S. Mukhopadhyay, "An energy-quality scalable wireless image sensor node for object-based video surveillance," *IEEE J. Emerg. Sel. Topics Circuits Syst.*, vol. 8, no. 3, pp. 591–602, Sep. 2018.

[24] M. De Gregorio and M. Giordano, "Change detection with weightless neural networks," in *Proc. IEEE Conf. Comput. Vis. Pattern Recognit. Workshops*, Jun. 2014, pp. 403–407.

[25] Y. A. U. Rehman, M. Tariq, and T. Sato, "A novel energy efficient object detection and image transmission approach for wireless multimedia sensor networks," *IEEE Sensors J.*, vol. 16, no. 15, pp. 5942–5949, Aug. 2016.

[26] A. Aliouat, N. Kouadria, S. Harize, and M. Maimour, "Multi-threshold-based frame segmentation for content-aware video coding in WMSN," in *Proc. Int. Conf. Comput. Syst. Appl.* Cham, Switzerland: Springer, 2022, pp. 337–347.

[27] J. H. Ko, B. A. Mudassar, and S. Mukhopadhyay, "An energy-efficient wireless video sensor node for moving object surveillance," *IEEE Trans. Multi-Scale Comput. Syst.*, vol. 1, no. 1, pp. 7–18, Jan./Mar. 2015.

[28] A. Aliouat, N. Kouadria, M. Maimour, S. Harize, and N. Doghmane, "Region-of-interest based video coding strategy for rate/energy-constrained smart surveillance systems using WMSNs," *Ad Hoc Netw.*, vol. 140, Mar. 2023, Art. no. 103076.

[29] S. S. Sengar and S. Mukhopadhyay, "Motion segmentation-based surveillance video compression using adaptive particle swarm optimization," *Neural Comput. Appl.*, vol. 32, no. 15, pp. 11443–11457, Aug. 2020.

[30] W. Guo, C. Yan, and T. Lu, "Optimizing the lifetime of wireless sensor networks via reinforcement-learning-based routing," *Int. J. Distrib. Sensor Netw.*, vol. 15, no. 2, Feb. 2019, Art. no. 155014771983354.

[31] S. M. Chowdhury and A. Hossain, "Different energy saving schemes in wireless sensor networks: A survey," *Wireless Pers. Commun.*, vol. 114, no. 3, pp. 2043–2062, Oct. 2020.

[32] D. K. Sah and T. Amgoth, "Parametric survey on cross-layer designs for wireless sensor networks," *Comput. Sci. Rev.*, vol. 27, pp. 112–134, Feb. 2018.

[33] A. A. Youssif and A. Z. Ghalwash, "Energy aware and adapative cross layer scheme for video transmission over wireless sensor networks," *IEEE Sensors J.*, vol. 16, no. 21, pp. 7792–7802, Jun. 2016.

[34] O. Iqbal, V. I. T. Muro, S. Katoch, A. Spanias, and S. Jayasuriya, "Adaptive subsampling for ROI-based visual tracking: Algorithms and FPGA implementation," *IEEE Access*, vol. 10, pp. 90507–90522, 2022.

[35] I. M. Hameed, S. H. Abdulhussain, and B. M. Mahmmod, "Content-based image retrieval: A review of recent trends," *Cogent Eng.*, vol. 8, no. 1, Jan. 2021, Art. no. 1927469.

[36] M. Fularz, M. Kraft, A. Schmidt, and A. Kasiński, "A high-performance FPGA-based image feature detector and matcher based on the FAST and BRIEF algorithms," *Int. J. Adv. Robotic Syst.*, vol. 12, no. 10, p. 141, Oct. 2015.

[37] P. Kumar, A. Singhal, S. Mehta, and A. Mittal, "Real-time moving object detection algorithm on high-resolution videos using GPUs," *J. Real-Time Image Process.*, vol. 11, no. 1, pp. 93–109, 2016.

[38] K. Goyal and J. Singhai, "Review of background subtraction methods using Gaussian mixture model for video surveillance systems," *Artif. Intell. Rev.*, vol. 50, no. 2, pp. 241–259, 2018.

[39] K. Kim, T. H. Chalidabhongse, D. Harwood, and L. Davis, "Real-time foreground–background segmentation using codebook model," *Real-Time Imag.*, vol. 11, no. 3, pp. 172–185, 2005.

[40] O. Barnich and M. Van Droogenbroeck, "ViBe: A universal background subtraction algorithm for video sequences," *IEEE Trans. Image Process.*, vol. 20, no. 6, pp. 1709–1724, Jun. 2011.

[41] R. Antonio, S. Faria, L. M. N. Tavora, A. Navarro, and P. Assuncao, "Learning-based compression of visual objects for smart surveillance," in *Proc. 11th Int. Conf. Image Process. Theory, Tools Appl. (IPTA)*, Apr. 2022, pp. 1–6.
[42] H. Zhu, X. Yan, H. Tang, Y. Chang, B. Li, and X. Yuan, "Moving object detection with deep CNNs," *IEEE Access*, vol. 8, pp. 29729–29741, 2020.
[43] S. S. Sengar and S. Mukhopadhyay, "Moving object detection based on frame difference and W4," *Signal, Image Video Process.*, vol. 11, no. 7, pp. 1357–1364, Oct. 2017.
[44] S. H. Shaikh, K. Saeed, and N. Chaki, "Moving object detection using background subtraction," in *Moving Object Detection Using Background Subtraction*. Cham, Switzerland: Springer, 2014, pp. 15–23.
[45] A. Haidous, W. Oswald, H. Das, and N. Gong, "Content-adaptable ROI-aware video storage for power-quality scalable mobile streaming," *IEEE Access*, vol. 10, pp. 26830–26848, 2022.
[46] B. Li, L. Ye, J. Liang, Y. Wang, and J. Han, "Region-of-interest and channel attention-based joint optimization of image compression and computer vision," *Neurocomputing*, vol. 500, pp. 13–25, Aug. 2022.
[47] G. Wu, M. Qin, T. M. Bae, S. Li, Y. Fang, and Y.-K. Chen, "Region of interest quality controllable video coding techniques," U.S. Patent 11 277 626, Mar. 15, 2022.
[48] D. Min, S. Choi, J. Lu, B. Ham, K. Sohn, and M. Do, "Fast global image smoothing based on weighted least squares," *IEEE Trans. Image Process.*, vol. 23, no. 12, pp. 5638–5653, Dec. 2014.
[49] N. R. Harvey and S. Marshall, "Rank-order morphological filters: A new class of filters," in *Proc. IEEE Workshop Nonlinear Signal Image Process.*, 1995, pp. 975–978.
[50] Y. Wang, P.-M. Jodoin, F. Porikli, J. Konrad, Y. Benezeth, and P. Ishwar, "CDnet 2014: An expanded change detection benchmark dataset," in *Proc. IEEE Conf. Comput. Vis. Pattern Recognit. Workshops*, Jun. 2014, pp. 387–394.
[51] Z. Zivkovic and F. Van Der Heijden, "Efficient adaptive density estimation per image pixel for the task of background subtraction," *Pattern Recognit. Lett.*, vol. 27, no. 7, pp. 773–780, 2006.
[52] C. Stauffer and W. E. L. Grimson, "Adaptive background mixture models for real-time tracking," in *Proc. IEEE Comput. Soc. Conf. Comput. Vis. Pattern Recognit.*, vol. 2. Jun. 1999, pp. 246–252.
[53] A. Elgammal, D. Harwood, and L. Davis, "Non-parametric model for background subtraction," in *Proc. Eur. Conf. Comput. Vis.* Cham, Switzerland: Springer, 2000, pp. 751–767.
[54] Y. Benezeth, P.-M. Jodoin, B. Emile, H. Laurent, and C. Rosenberger, "Comparative study of background subtraction algorithms," *J. Electron. Imag.*, vol. 19, no. 3, Jul. 2010, Art. no. 033003.
[55] Z. Zivkovic, "Improved adaptive Gaussian mixture model for background subtraction," in *Proc. 17th Int. Conf. Pattern Recognit.*, vol. 2, 2004, pp. 28–31.
[56] M. F. Savaş, H. Demirel, and B. Erkal, "Moving object detection using an adaptive background subtraction method based on block-based structure in dynamic scene," *Optik*, vol. 168, pp. 605–618, Sep. 2018.
[57] Arm. (2018). *Cortex M3 Datasheet*. [Online]. Available: https://iot-lab.github.io/assets/misc/docs/iot-lab-m3/stm32f103re.pdf
[58] Y. Shen, W. Hu, J. Liu, M. Yang, B. Wei, and C. T. Chou, "Efficient background subtraction for real-time tracking in embedded camera networks," in *Proc. 10th ACM Conf. Embedded Netw. Sensor Syst.*, Nov. 2012, pp. 295–308.
[59] Y. Shen, W. Hu, M. Yang, J. Liu, B. Wei, S. Lucey, and C. T. Chou, "Real-time and robust compressive background subtraction for embedded camera networks," *IEEE Trans. Mobile Comput.*, vol. 15, no. 2, pp. 406–418, Feb. 2016.
[60] M. U. K. Khan, A. Khan, and C.-M. Kyung, "EBSCam: Background subtraction for ubiquitous computing," *IEEE Trans. Very Large Scale Integr. (VLSI) Syst.*, vol. 25, no. 1, pp. 35–47, May 2016.
[61] D.-U. Lee, H. Kim, M. Rahimi, D. Estrin, and J. D. Villasenor, "Energy-efficient image compression for resource-constrained platforms," *IEEE Trans. Image Process.*, vol. 18, no. 9, pp. 2100–2113, Sep. 2009.

AHCEN ALIOUAT (Student Member, IEEE) received the bachelor's and master's degrees in telecommunication, networks, and multimedia from the Telecommunication Department, University of Sciences and Technology Houari Boumediene (USTHB), Algeria, in 2016 and 2018, respectively. He is currently pursuing the Ph.D. degree in multimedia and digital communications with the Electronics Department, Badji Mokhtar–Annaba University (UBMA), Algeria. His research interests include image and video coding, signal processing, digital communications, and artificial intelligence. His Ph.D. work interests include video/image coding and transmission over wireless networks with resource constraints.

NASREDDINE KOUADRIA received the Ph.D. and Habilitation degrees in multimedia and digital communication from Badji Mokhtar–Annaba University, Algeria, in 2014 and 2018, respectively. He was a Postdoctoral Research Associate with the Technical University of Iasi, Romania, in 2019. He is currently a Senior Lecturer with the Department of Electronics, Annaba University, and a Research Member of the Laboratory of Automation and Signals of Annaba (LASA). His research interests include WSNs, image/video coding, fast transformations, communication, and digital signal processing.

SALIHA HARIZE received the Ph.D. and Habilitation degrees from Badji Mokhtar–Annaba University, Algeria, in 2014 and 2017, respectively. She is currently a Senior Lecturer and a member of the Laboratory of Automatic and Signal Processing of Annaba (LASA). Her research interests include image and video compression and the implementation of digital circuits on FPGA and cryptography.

MOUFIDA MAIMOUR received the engineering degree in computer science from the University of Constantine, Algeria, in 1998, and the Ph.D. degree from Claude Bernard University, in 2003. She has been a member of the Centre de Recherches en Automatique de Nancy (CRAN), since 2004. She is currently an Associate Professor with Lorraine University, Nancy, France. She conducted her doctoral research with the Laboratoire Informatique du Parralélisme (LIP), ENS Lyon, France. She mainly worked on reliable multicast and congestion control on the internet and took part in multiple networking and grid computing projects. Her current research interests include wireless sensor networks, knowledge-defined networks, and digital twining for the IoT, with a focus on the Industrial Internet of Things (IIoT) and the Internet of Multimedia Things (IoMT). Her machine-learning algorithms are leveraged to solve issues related to Industry 4.0 in the former and to multimedia environment surveillance in the latter.